Deuteron-Model Calculation of the High-Energy Nuclear Photoeffect*

K. G. Dedrick
Stanford University, Stanford, California

(Received May 6, 1955)

The high-energy nuclear photoeffect has been calculated according to the "deuteron model" of Levinger. In this model, the photoprocess occurs when a neutron and a proton which are scattering one another inside the nucleus absorb the energy of the incident photon and escape from the nuclear potential well into the laboratory. The nuclear photoeffect cross section is then obtained by averaging the cross section for the above process over all possible neutron-proton pairs in the nucleus, assuming a nucleon momentum distribution. The electric dipole and quadrupole interactions of the radiation field with the neutron and proton are included, and the magnetic terms are neglected. The averaging over all neutron-proton pairs is performed by means of a random flight formulation of the problem. The analytical work involved may conveniently be done using either a zero-temperature Fermi ground-state nucleon momentum distribution or a Gaussian distribution. Numerical results for the energy and angle distributions of photoneutrons and photoprotons are presented in the case of the Gaussian distribution, for four photon energies between 50 and 125 Mev.

I. INTRODUCTION

LEVINGER'S[1] deuteron model for the high-energy nuclear photoeffect has been sufficiently successful in interpreting experimental data to warrant further calculations. This model assumes as a photon absorption process, the photodissociation of a neutron and a proton within the nucleus which interact through a short range potential and are scattering one another.[2] The neutron and proton absorb the photon energy and may then escape from the nucleus. The nuclear photoeffect cross section is obtained by averaging the cross section for the photodissociation of the quasi-deuteron over all possible neutron-proton pairs in the nucleus. Corrections may be made to this result for the scattering of the prospective photoparticle by other nucleons in the nucleus and consideration given to the effects of the Coulomb and centrifugal barriers at the nuclear surface.

Levinger[1] shows that the cross section for the photodissociation of the quasi-deuteron can be related to the cross section for the bound deuteron, and makes use of the deuteron photoeffect cross sections calculated by Schiff[3] and by Marshall and Guth.[4] We calculate instead the photodissociation cross section of a neutron and proton which are scattering one another and confined to a volume v which is later taken to be the volume of the nucleus under consideration. For initial and final state wave functions, triplet n-p scattering wave functions are fabricated to provide agreement with the phenomenological low-energy n-p interaction. Only the electric dipole and electric quadrupole contributions are calculated. The magnetic terms are neglected because they are expected to be small, and furthermore their neglect does not distort the angular dependence of the cross section in that there is no interference with the electric terms.

Deuteron-model calculations in the past[1,5] have handled the averaging over all quasi-deuterons in a manner which does not yield an analytical result. This average is dependent on the nuclear ground-state neutron and proton momentum distributions. Levinger assumes Fermi distributions with a temperature of 8 Mev, and Weil and McDaniel[5] use zero-temperature Fermi distributions.

The averaging is handled here by interpreting the kinematics as a random-flight problem involving the sum of four momentum vectors. It is necessary to choose ground-state nucleon momentum distributions that will submit to the repeated integrations which arise in the random-flight theory. The zero-temperature Fermi distribution and the Gaussian are satisfactory in this respect, and the averaging is performed for both. The analyses of other types of nuclear experiments like the "pickup" process[6] and the nuclear scattering of 320-Mev protons[7] suggest that the Fermi distribution does not give as good agreement with experiment as do smoother distributions. The distribution proportional[8] to $(p^2+a^2)^{-2}$, where p is the nucleon momentum and a^2 corresponds to 18 Mev, is found to give reasonable agreement with the "pickup" process experiments,[9] but does not give as good agreement with the proton scattering experiments[7] as does a Gaussian distribution with a $1/e$ value of 16 Mev. In view of this, numerical evaluation of the photoeffect calculation presented below has been done only in the case of the Gaussian momentum distribution.

Corrections for the collisions of the photoparticles with other nucleons inside the nucleus have not been included here. This effect mainly influences the low-

* Supported in part by the Office of Scientific Research, Air Research and Development Command.

[1] J. S. Levinger, Phys. Rev. 84, 43 (1951).
[2] In Levinger's terminology, such a neutron and proton are referred to as a "quasi-deuteron."
[3] L. I. Schiff, Phys. Rev. 78, 733 (1950).
[4] J. F. Marshall and E. Guth, Phys. Rev. 78, 738 (1950).
[5] J. W. Weil and B. C. McDaniel, Phys. Rev. 92, 391 (1953).
[6] G. F. Chew and M. L. Goldberger, Phys. Rev. 77, 470 (1950).
[7] Cladis, Hess, and Moyer, Phys. Rev. 87, 425 (1952).
[8] This is the "Chew-Goldberger" distribution. See reference 6.
[9] H. York, Phys. Rev. 75, 1467(A) (1949).

energy photoparticles as the mean free path of a nucleon in nuclear matter is shorter for low-energy nucleons.[10]

In Sec. IV, account is taken of the reflections of photoneutrons from the edge of the nucleus where we expect a rapid change in nuclear potential and also a centrifugal barrier corresponding to the angular momentum of the photoneutron. In the case of photoprotons, the effect of the Coulomb barrier in reducing the penetration probability is also considered.

Tables of the numerical work are presented for photon energies of 50, 75, 100, and 125 Mev. These tables are not corrected for nuclear surface barrier penetrability, as it is necessary to specify a particular nucleus in calculating the penetrability. Directions for using the tables for a particular nucleus are presented in Sec. V.

II. QUASI-DEUTERON PHOTODISSOCIATION CROSS SECTION

The neutron and proton comprising the quasi-deuteron are assumed to interact through a short-range static potential of the kind usually assumed in explanations of the deuteron ground state and the low-energy n-p scattering. By virtue of this interaction, the neutron and proton can recoil against one another and absorb the energy of the photon. A direct calculation shows that without the n-p interaction, the cross section for the photon absorption is zero.

This calculation is very similar to the deuteron photoeffect calculations where one calculates the transition probability per unit time per unit incident photon flux from the deuteron ground state to a final state where the neutron and proton are nearly free, but still interact through the n-p potential. Just as in the deuteron photoeffect calculation, we obtain:

$$\sigma(\theta)=\frac{\sin^2\theta}{8\pi}[3\sigma_d+6(5\sigma_d\sigma_q)^{\frac{1}{2}}\cos\theta\cos\delta_2+15\sigma_q\cos^2\theta], \quad (1)$$

where

$$\sigma_d=\frac{4\pi^2}{3}\left(\frac{e^2}{\hbar c}\right)\frac{Mk_fE_\gamma'}{\hbar^2}|I_1|^2,$$
$$\sigma_q=\frac{\pi^2}{60}\left(\frac{e^2}{\hbar c}\right)\frac{Mk_f(E_\gamma')^3}{\hbar^4c^2}|I_2|^2; \quad (2)$$

θ is the angle of the photoparticle with respect to the direction of the incident photon, σ_d and σ_q are respectively the total electric dipole and electric quadrupole cross sections, M is the nucleon mass, k_f is the final nucleon momentum, E_γ' is the photon energy seen in the center-of-mass system, and

$$I_1\equiv\int_0^\infty R_1^*(r)r^3\psi_i(r)dr,$$
$$I_2\equiv\int_0^\infty R_2^*(r)r^4\psi_i(r)dr. \quad (3)$$

In these expressions for I_1 and I_2, $R_1(r)$ is the radial part of the p state contribution to the final state wave function and $R_2(r)$ is the same for the d state. These final state radial functions are normalized to have the asymptotic form $R_l(r)\rightarrow\cos\delta_l\, j_l(k_fr)-\sin\delta_l\, n_l(k_fr)$, where the δ_l are the phase shifts.[11] In calculating the $R_l(r)$, we shall use the Serber force[12] which yields an interaction only for even values of l. This gives us the result that $R_l(r)=j_l(k_fr)$ for odd l. In calculating I_2, the r^4 factor in the integrand makes the details of $R_2(r)$ unimportant near $r=0$. Because of this, we use the asymptotic form[13]

$$R_2(r)\rightarrow\cos\delta_2\, j_2(k_fr)-\sin\delta_2\, n_2(k_fr).$$

The phase shift δ_2 is calculated by the Born approximation.[14]

For the initial state wave function ψ_i, we use the $l=0$ part of the n-p wave function in the triplet n-p potential. Neglect of the singlet interaction is not felt to be serious and considerably simplifies the calculation. Rather than start with the n-p potential where in general it is impossible to solve the wave equation, we make a choice for ψ_i which correctly gives the low-energy n-p scattering and in the limit of a negative value for the relative energy, becomes the deuteron bound-state solution for the Hulthén potential. This wave function is:

$$\psi_i(r)=(A/r)u_i(r)$$

where

$$u_i(r)=\frac{\sin(k_ir+\delta_0)}{\sin\delta_0}-e^{-\beta r}.$$

From the "effective range" theories of Bethe[15] and Schwinger,[16] we use

$$k_i\cot\delta_0\cong-1/a_t+\tfrac{1}{2}r_{0t}k_i^2.$$

The effective range is r_{0t}, and a_t is the triplet scattering length. The parameter β is given by[17,18]

$$\beta=\frac{3}{2r_{0t}}\left[1+\left(1-\frac{16}{9}\frac{r_{0t}}{a_t}\right)^{\frac{1}{2}}\right].$$

Following Levinger, we choose the normalization factor A so that ψ_i is the s wave part of a plane wave Ψ_i which is normalized so that it yields one n-p pair in a volume v which is later taken to be the volume of the

[10] Weil and McDaniel[5] show how collisions affect the photoparticle energy spectra.

[11] L. I. Schiff, *Quantum Mechanics* (McGraw-Hill Book Company, Inc , New York, 1949), Chap. V, Sec. 19.

[12] J. M. Blatt and V. F. Weisskopf, *Theoretical Nuclear Physics* (John Wiley and Sons, Inc., New York, 1952), p. 179.

[13] This approximation is used in references 3 and 4.

[14] Reference 11, p. 165.

[15] H. A. Bethe, Phys. Rev. **76**, 38 (1949).

[16] J. Schwinger, Phys. Rev. **72**, 742(A) (1947).

[17] A justification for using this formula for β is presented in the dissertation by the author, copies of which may be obtained from University Microfilms, 313 N. 1st St. Ann Arbor, Michigan. (Cat. No. 11171) (unpublished).

[18] Recent experiment shows $r_{0t}=1.7\times10^{-13}$ cm, $a_t=5.39\times10^{-13}$ cm. (See reference 12, p. 71.)

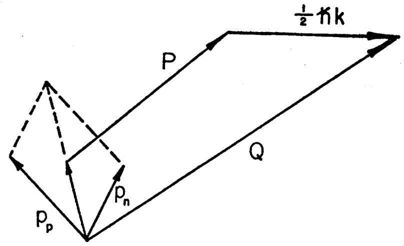

FIG. 1. The vector composition of the photoparticle momentum **Q**.

nucleus under consideration. This gives the result $A=v^{-\frac{1}{2}}\sin\delta_0$.

The results of calculation of I_1 and I_2 by Eq. (3) are lengthy algebraic expressions and are not included here.[19] The cross sections σ_d and σ_q follow directly through Eq. (2).

III. AVERAGING PROCESS

The averaging over-all quasi-deuterons is complicated by the dependence of the quasi-deuteron photodissociation cross section on the relative momentum of the neutron and proton, and on the photon energy that appears in the quasi-deuteron center of mass. This photon energy is given by a Doppler shift from the energy of the incident radiation and is dependent on the motion of the quasi-deuteron center of mass in the nucleus. The averaging is performed by interpreting the situation as a random flight problem involving four vectors. The momentum vector **Q** of a photoparticle in the laboratory is given by[20]

$$\mathbf{Q}=\mathbf{P}+\tfrac{1}{2}(\mathbf{p}_n+\mathbf{p}_p)+\tfrac{1}{2}\hbar\mathbf{k}. \tag{4}$$

The vector $(\mathbf{p}_n+\mathbf{p}_p)$ in Eq. (4) or Fig. 1, is the momentum of the center of mass of the quasi-deuteron, where $\mathbf{p}_n$ is the neutron momentum and $\mathbf{p}_p$ is the proton momentum. One-half of this must be added to **P**, the momentum of the photoneutron or photoproton taken in the center-of-mass frame. In addition, each photoparticle receives a contribution $\frac{1}{2}\hbar\mathbf{k}$. We are interested in obtaining a distribution function which gives the probability $W(\mathbf{Q})d\mathbf{Q}$ that **Q** lies in the range $dQ_xdQ_ydQ_z \equiv d\mathbf{Q}$ about **Q**.

The center-of-mass frame for the quasi-deuteron photodissociation will be taken as the quasi-deuteron center of mass. This means that the effect of the photon momentum in establishing the frame of reference is being neglected.

The random flight formulation consists in treating the momentum vectors in Eq. (4) as random variables. Chandrasekhar[21] gives the solution to random flight problems in a form convenient for our use. The calculation has been carried out in two steps. Let us take $\mathbf{Q}=\mathbf{Q}'-\frac{1}{2}\hbar\mathbf{k}$, where $\mathbf{Q}'=\mathbf{P}+\frac{1}{2}(\mathbf{p}_n+\mathbf{p}_p)$. We first calculate $W'(\mathbf{Q}')$ according to the random flight formalism, and then calculate $W(\mathbf{Q})$ by a reapplication of the same formalism. $W'(\mathbf{Q}')$ is given by[21]

$$W'(\mathbf{Q}')=\frac{1}{8\pi^3}\int \exp(-i\boldsymbol{\varrho}\cdot\mathbf{Q}')A'(\boldsymbol{\varrho})d\boldsymbol{\varrho}, \tag{5a}$$

where

$$A'(\boldsymbol{\varrho}')=\int\int\int \exp[i\boldsymbol{\varrho}\cdot(\mathbf{p}+\mathbf{q}_n+\mathbf{q}_p)]\tau_P(E_\gamma,\mathbf{q}_n,\mathbf{q}_p,\mathbf{P}) \times\tau_n(\mathbf{q}_n)\tau_p(\mathbf{q}_p)d\mathbf{P}d\mathbf{q}_nd\mathbf{q}_p, \tag{5b}$$

with $\mathbf{q}_n=\frac{1}{2}\mathbf{p}_n$ and $\mathbf{q}_p=\frac{1}{2}\mathbf{p}_p$. Similarly, $W(\mathbf{Q})$ is obtained from $W'(\mathbf{Q}')$:

$$W(\mathbf{Q})=\frac{1}{8\pi^3}\int \exp(-i\boldsymbol{\varrho}\cdot\mathbf{Q})A(\boldsymbol{\varrho})d\boldsymbol{\varrho}, \tag{6a}$$

$$A(\boldsymbol{\varrho})=\int \exp(i\boldsymbol{\varrho}\cdot\mathbf{p}_k)\tau_k(\mathbf{p}_k)d\mathbf{p}_k \times\int \exp(i\boldsymbol{\varrho}\cdot\mathbf{Q}')W'(\mathbf{Q}')d\mathbf{Q}', \tag{6b}$$

where we have introduced $\mathbf{p}_k=\frac{1}{2}\hbar\mathbf{k}$.

Knowledge of $W(\mathbf{Q})$ gives us not only the angular distribution of photoparticles but the energy distribution as well. Let us take Θ and Φ as the polar angles for the vector **Q**. Then $d\mathbf{Q}$ is given by $dQ=Q^2dQd\Omega$, where $d\Omega=\sin\Theta d\Phi d\Theta$ is the element of solid angle in **Q** space. Further, since the energy of the photoparticle above the bottom of the nuclear well is given nonrelativistically by $E_w=Q^2/(2M)$, we have

$$W(\mathbf{Q})d\mathbf{Q}=W(\mathbf{Q})(2M^3E_w)^{\frac{1}{2}}dE_wd\Omega. \tag{7}$$

The cross section $\sigma(\Theta,\Phi,E_w)$ per unit solid angle per unit energy of the photoparticle is then

$$\sigma(\Theta,\Phi,E_w)=W(\mathbf{Q})(2M^3E_w)^{\frac{1}{2}}. \tag{8}$$

If the depth of the nuclear potential well is V, the energy of the photoparticles in the laboratory is given by $E_L=E_w-V$. After the cross section $\sigma(\Theta,\Phi,E_w)$ is evaluated according to Eq. (8), the photoparticle energy scale must be shifted by an amount V which may be chosen from the analysis by Adair[22] of the results of neutron scattering experiments or on some other basis.

In calculating $W'(\mathbf{Q}')$ according to Eq. (5), we require the probability density $\tau_P(E_\gamma,\mathbf{q}_n,\mathbf{q}_p,\mathbf{P})$, given the values of E_γ, $\mathbf{q}_n$, and $\mathbf{q}_p$, that **P** will lie in the range $d\mathbf{P}$ about **P**. The quasi-deuteron photodissociation cross section calculated in the previous section according to (1) and (2), may be written

$$\sigma_{np}(|\mathbf{p}_n-\mathbf{p}_p|,E_\gamma',\theta_P)$$

[19] See reference 17, pp. 37–38.

[20] Equation (4) is not quite correct for relativistic particle energies (i.e., for photon energies that are a sizable fraction of the nucleon rest energy). The approximation made in using Eq. (4) is consistent with others made in this work. A detailed development is presented in reference 17, in the Appendix, Sec. B.

[21] S. Chandrasekhar, Revs. Modern Phys. **15**, 8 (1943).

[22] Robert K. Adair, Phys. Rev. **94**, 737 (1954). A well depth of 40 Mev is suggested by this analysis.

where θ_P is the angle of the photoparticle in the quasi-deuteron center-of-mass system and E_γ' is the photon energy in the center-of-mass system. The cross section is dependent on the magnitude of $(\mathbf{p}_n-\mathbf{p}_p)$ and not on the direction since only the $l=0$ partial wave is included in the initial state wave function (moderate nucleon momenta). On multiplying σ_{np} by a delta function normalized to unity, which expresses conservation of energy in the photoprocess, we obtain τ_P.

$$\tau_P=\sigma_{np}\delta(|\mathbf{P}|-P_0)/P_0^2. \tag{9}$$

P_0 is the magnitude of the photoparticle momentum in the center of mass and is given by energy conservation between E_γ' and the initial relative energy between the neutron and proton. If we use the nonrelativistic Doppler formula to express E_γ' in terms of E_γ and introduce

$$\begin{aligned}\mathbf{r}&=\mathbf{q}_n-\mathbf{q}_p,\\ \mathbf{R}&=\mathbf{q}_n+\mathbf{q}_p,\end{aligned} \tag{10}$$

we find

$$P_0=\left[ME_\gamma\left(1-\frac{|\mathbf{R}|}{Mc}\cos\theta_R\right)+|\mathbf{r}|^2\right]^{\frac{1}{2}}. \tag{11}$$

Since σ_{np} depends on $\mathbf{r}$ through $|\mathbf{r}|$, and on $\mathbf{R}$ through the Doppler formula, it is seen that

$$\tau_P=\tau_P(|\mathbf{r}|,\mathbf{R},E_\gamma,\theta_P).$$

This suggests that the integrations indicated in (5) over $\mathbf{q}_n$ and $\mathbf{q}_p$ would be more easily performed if a transformation were made to the variables $\mathbf{r}$ and $\mathbf{R}$ as is Eq. (10). To do this, $\tau_n(\mathbf{q}_n)\tau_p(\mathbf{q}_p)d\mathbf{q}_nd\mathbf{q}_p$ must be replaced by $\tau_r(\mathbf{r})\tau_R(\mathbf{R})d\mathbf{r}d\mathbf{R}$. If τ_n and τ_p are of simple analytic form, this latter transformation is readily performed. τ_n and τ_p are closely related to the ground-state nucleon momentum distributions. The cross section σ_{np} may be expressed as a series of Legendre polynomials of order from zero to five in the angles of $\mathbf{P}$. The integration indicated in Eq. (5b) over these angles is readily carried out,[23] as is also the integration over P. The integration over the angles of $\mathbf{R}$ is complicated by the dependence of P_0 on θ_R as in Eq. (11) and the dependence of σ_{np} on E_γ' which is also a function of θ_R. A series expansion is made in powers of $(R\cos\theta_R)$ of σ_{np} and $j_n(\rho P_0)$ where the quadratic and higher terms are neglected.[24] Integration over θ_R then proceeds according to the same method used in the case of the angles of $\mathbf{P}$. Integration over the angles of $\mathbf{r}$ and $\boldsymbol{\varrho}$ is done by using the results quoted in footnote 23.

[23] This integration, and many others to be done, make use of

$$\int \exp(i\mathbf{k}\cdot\mathbf{r})P_n(\cos\theta_r)d\Omega_r=4\pi i^nP_n(\cos\theta_k)j_n(kr).$$

Of occasional use also is

$$\int_0^\infty j_n(\alpha\rho)j_n(\beta\rho)\rho^2d\rho=\frac{\pi}{2\alpha\beta}[\delta(\alpha-\beta)+(-1)^{n+1}\delta(\alpha+\beta)].$$

[24] A justification for this approximation is given in reference 17, Appendix D.

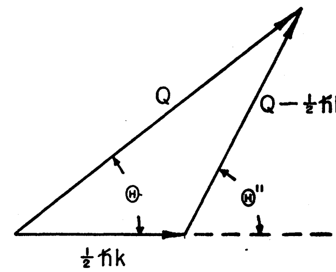

FIG. 2. Geometrical relation between Θ and Θ''.

The resulting expression for $W'(\mathbf{Q}')$ has yet to be integrated over r, R, and ρ, but first, specific forms for the ground state nucleon momentum distributions must be assumed. The integrations over R and ρ may be done by using the zero-temperature Fermi distribution and the Gaussian distribution. The result for $W'(\mathbf{Q}')$ is expressible in a series of Legendre polynomials. The coefficients in the case of the Gaussian distribution contain Gauss functions and Bessel functions of half-odd-integer order with an imaginary argument; in the case of the Fermi distribution, the coefficients are lengthy algebraic expressions. The integration over r is not done exactly, but is conveniently approximated numerically.

$W'(\mathbf{Q}')$ may be written

$$W'(\mathbf{Q}')=\sum_{n=0}^{5}B_n(|\mathbf{Q}'|)P_n(\cos\Theta'). \tag{12}$$

Next, $W(\mathbf{Q})$ must be obtained according to Eq. (6). For $\tau_k(\mathbf{p}_k)$ in Eq. (6b), we use $\delta(p_{kx})\delta(p_{ky})\delta(p_{kz}-\frac{1}{2}\hbar k)$, and readily obtain:

$$W(\mathbf{Q})=\sum_{n=0}^{5}B_n(|\mathbf{Q}-\tfrac{1}{2}\hbar\mathbf{k}|)P_n(\cos\Theta''), \tag{13}$$

where

$$|\mathbf{Q}-\tfrac{1}{2}\hbar\mathbf{k}|=Q[1+(\tfrac{1}{2}\hbar k/Q)^2-2(\tfrac{1}{2}\hbar k/Q)\cos\Theta]^{\frac{1}{2}}, \tag{14}$$

and

$$\cos\Theta''=\frac{\cos\Theta-(\frac{1}{2}\hbar k/Q)}{[1+(\frac{1}{2}\hbar k/Q)^2-2(\frac{1}{2}\hbar k/Q)\cos\Theta]^{\frac{1}{2}}}. \tag{15}$$

Figure 2 shows the geometrical relation between these quantities. Equation (13) states that to calculate $W(\mathbf{Q})$ for a given laboratory angle Θ and laboratory momentum Q with an associated energy E_w, we must calculate $\cos\Theta''$ and $|\mathbf{Q}-\frac{1}{2}\hbar\mathbf{k}|$ according to Eqs. (14) and (15) and substitute them into Eq. (13). The cross section $\sigma(\Theta,E_w)$ is then given by multiplying this result by $(2M^3E_w)^{\frac{1}{2}}$ as in Eq. (8). Numerical results in Table I are discussed in Sec. V.

IV. COULOMB AND CENTRIFUGAL BARRIER PENETRABILITIES

We assume that if a prospective photoparticle does not get through the Coulomb and centrifugal barriers on its first encounter, it does not get a second chance

TABLE I. Photoparticle yields assuming a Gaussian initial nucleon momentum distribution. Tabulated values are v times $\sigma(E_w,\Theta)$, where v is the nuclear volume in cubic centimeters. All entries are to be multiplied by 10^{-70}. The cross section $\sigma(E_w,\Theta)$ then has the units: cm^2/Mev.

Photon energy Mev	E_w, Mev	Laboratory angle—degrees 10	20	30	40	50	60	70	80	90	100	110	120	130	140	150	160	170
										Photoprotons								
50	43.20	108.9	132.8	164.7	195.5	216.9	223.6	214.7	192.5	161.9	128.3	96.01	68.28	46.46	30.61	19.96	13.43	9.981
	53.33	86.06	107.0	134.5	160.4	177.5	181.6	172.4	152.5	126.3	98.38	72.40	50.55	33.65	21.52	13.41	8.422	5.776
	64.53	58.79	74.54	95.02	113.9	125.8	127.9	120.2	105.1	85.99	66.20	48.17	33.26	21.84	13.66	8.160	4.729	2.876
	76.80	34.56	44.80	57.99	69.91	77.14	77.98	72.73	63.03	51.13	39.08	28.27	19.44	12.69	7.822	4.495	2.374	1.203
	90.13	17.38	23.14	30.49	37.03	40.88	41.18	38.19	32.90	26.56	20.24	14.64	10.08	6.577	4.019	2.232	1.063	0.4036
	104.53	7.421	10.21	13.76	16.88	18.69	18.81	17.40	14.95	12.06	9.199	6.681	4.624	3.030	1.843	0.9935	0.4241	0.0963
										Photoneutrons								
	43.20	46.44	62.07	85.44	112.9	140.0	162.5	177.1	181.9	176.9	163.3	143.5	120.3	96.18	73.56	54.20	39.47	30.27
	53.33	36.25	49.36	68.68	90.89	112.2	129.2	139.3	141.4	135.9	124.1	108.0	89.53	70.78	53.32	38.45	27.13	20.07
	64.53	24.78	34.30	48.15	63.75	78.30	89.40	95.48	96.02	91.48	82.91	71.66	59.09	46.40	34.62	24.56	16.88	12.08
	76.80	14.79	20.77	29.36	38.85	47.47	53.79	56.99	56.90	53.91	48.68	41.98	34.56	27.07	20.08	14.07	9.468	6.572
	90.13	7.685	10.93	15.53	20.52	24.95	28.09	29.59	29.42	27.82	25.13	21.70	17.90	14.02	10.37	7.201	4.756	3.212
	104.53	3.470	4.983	7.105	9.373	11.35	12.72	13.36	13.27	12.57	11.40	9.890	8.188	6.427	4.745	3.272	2.126	1.400
										Photoprotons								
75	30.49	27.86	35.32	45.63	56.23	64.57	68.74	67.92	62.44	53.56	43.00	32.42	23.13	15.84	10.70	7.459	5.650	4.797
	37.65	34.75	44.46	57.62	70.65	80.17	83.90	81.15	72.78	60.72	47.25	34.43	23.64	15.51	9.999	6.660	4.873	4.065
	45.55	39.13	50.55	65.71	80.17	89.93	92.59	87.78	76.94	62.58	47.39	33.53	22.30	14.10	8.709	5.516	3.837	3.086
	54.21	39.70	51.84	67.61	82.10	91.10	92.34	85.91	73.74	58.64	43.39	29.98	19.44	11.96	7.110	4.259	2.746	2.053
	63.62	36.25	47.88	62.71	75.84	83.29	83.21	76.08	64.06	49.95	36.26	24.60	15.69	9.461	5.458	3.077	1.774	1.149
	73.79	29.73	39.91	52.39	63.14	68.70	67.71	60.93	50.44	38.68	27.65	18.54	11.70	6.986	3.939	2.085	1.026	0.4917
	84.71	21.84	29.70	39.37	47.35	51.09	49.75	44.13	35.99	27.23	19.25	12.82	8.067	4.800	2.664	1.325	0.5251	0.1021
	96.38	14.33	19.87	26.59	31.95	34.20	32.94	28.86	23.26	17.42	12.23	8.124	5.125	3.056	1.673	0.7547	0.1778	...
	108.80	8.348	11.88	16.09	19.36	20.61	19.67	17.06	13.62	10.13	7.091	4.718	2.994	1.327	0.7211	0.3044	0.0342	...
										Photoneutrons								
	30.49	8.364	12.62	19.61	28.92	39.70	50.64	60.13	66.67	69.26	67.62	62.24	54.16	44.70	35.15	26.63	19.99	15.80
	37.65	9.813	15.07	23.54	34.55	46.89	58.87	68.62	74.57	75.85	72.50	65.32	55.62	44.86	34.37	25.24	18.23	13.84
	45.55	10.57	16.49	25.86	37.73	50.56	62.44	71.43	76.10	75.88	71.12	62.88	52.57	41.61	31.22	22.32	15.56	11.36
	54.21	10.40	16.48	25.90	37.52	49.63	60.28	67.71	70.79	69.31	63.86	55.58	45.80	35.73	26.38	18.46	12.48	8.775
	63.62	9.327	14.98	23.58	33.89	44.24	52.87	58.36	59.97	57.77	52.48	45.12	36.79	28.42	20.74	14.27	9.403	6.382
	73.79	7.603	12.29	19.47	27.75	35.75	42.06	45.68	46.23	43.94	39.47	33.64	27.25	20.92	15.14	10.29	6.632	4.359
	84.71	5.628	9.243	14.55	20.56	26.15	30.32	32.45	32.41	30.47	27.16	23.03	18.59	14.22	10.24	6.893	4.360	2.783
	96.38	3.781	6.258	9.828	13.75	17.26	19.73	20.86	20.64	19.27	17.10	14.47	11.67	8.914	6.390	4.237	2.602	1.581
	108.80	2.303	3.830	5.992	8.300	10.28	11.61	12.16	11.94	11.11	9.846	8.336	6.725	3.795	2.711	1.781	1.074	0.6319
										Photoprotons								
100	23.56	2.837	4.075	5.923	8.069	10.12	11.68	12.44	12.24	11.16	9.446	7.439	5.491	3.864	2.683	1.994	1.554	1.387
	29.09	4.846	6.860	9.786	13.04	15.96	17.90	18.47	17.56	15.42	12.50	9.389	6.574	4.373	2.890	2.048	1.663	1.534
	35.20	7.548	10.58	14.88	19.47	23.27	25.42	25.46	23.42	19.82	15.44	11.09	7.376	4.638	2.909	2.007	1.653	1.571
	41.89	10.74	14.98	20.83	26.79	31.35	33.40	32.52	29.00	23.72	17.81	12.27	7.787	4.642	2.755	1.834	1.513	1.466
	49.16	13.99	19.47	26.82	33.99	39.00	40.58	38.46	33.31	26.41	19.17	12.74	7.763	4.413	2.477	1.565	1.260	1.221
	57.02	16.71	23.24	31.80	39.76	44.78	45.57	42.12	35.49	27.34	19.27	12.41	7.326	4.008	1.870	1.252	0.9386	0.8765
	65.45	18.30	25.50	34.71	42.86	47.45	47.28	42.67	35.06	25.57	18.07	11.36	6.554	3.492	1.865	0.9412	0.6071	0.5052
	74.47	18.38	25.73	34.88	42.61	46.41	45.33	40.00	32.10	23.53	15.82	9.769	5.555	2.918	1.429	0.6686	0.3194	0.1793
	84.07	16.93	23.85	32.27	39.04	41.88	40.14	34.68	27.23	19.56	12.91	7.880	4.457	1.887	1.113	0.4507	0.1087	...
	94.25	14.29	20.31	27.48	32.96	34.86	32.82	27.81	21.40	15.10	9.833	5.960	3.375	1.776	0.8328	0.2895	...	...
	105.02	11.02	15.87	21.51	25.62	26.75	24.78	20.61	15.58	10.82	6.980	4.222	2.407	1.279	0.5941	0.1778	...	...
	116.36	7.747	11.36	15.47	18.33	18.92	17.26	14.12	10.51	7.208	4.618	2.798	1.627	0.8662	0.4004	0.1044	...	...

TABLE I.—(*Continued*).

Photon energy Mev	E_w, Mev	Laboratory angle—degrees 10	20	30	40	50	60	70	80	90	100	110	120	130	140	150	160	170
									Protoprotons—*Continued*									
100	128.29	4.937	7.423	10.20	12.05	12.32	11.09	8.941	6.563	4.458	2.846	1.733	1.009	0.5492	0.2532	0.0585	...	...
	140.80	2.829	4.411	6.150	7.267	7.374	6.564	5.227	3.795	2.560	1.634	1.002	0.5903	0.3247	0.1493	0.0312	...	...
	153.89	1.436	2.367	3.378	4.010	4.052	3.575	2.820	2.031	1.365	0.8737	0.5401	0.3218	0.1799	0.0818	0.0158	...	...
										Photoneutrons								
	23.56	0.6483	1.258	2.416	4.261	6.845	10.04	13.51	16.73	19.15	20.33	20.11	18.60	16.17	13.30	10.49	8.171	6.651
	29.09	0.9217	1.823	3.506	6.125	9.695	13.97	18.42	22.32	24.95	25.85	24.93	22.47	19.00	15.16	11.54	8.625	6.751
	35.20	1.252	2.522	4.840	8.349	12.98	18.31	23.60	27.90	30.43	30.75	28.92	25.41	20.94	16.24	11.96	8.597	6.463
	41.89	1.602	3.290	6.296	10.71	16.32	22.52	28.31	32.66	34.73	34.23	31.43	26.98	21.71	16.42	11.75	8.135	5.870
	49.16	1.917	4.018	7.669	12.85	19.20	25.88	31.75	35.71	37.05	35.67	32.03	26.92	21.23	15.72	10.30	7.341	5.086
	57.02	2.137	4.576	8.711	14.39	21.06	27.74	33.21	36.45	36.94	34.79	30.62	25.29	19.62	14.46	9.756	6.339	4.222
	65.45	2.216	4.851	9.203	14.99	21.50	27.68	32.36	34.69	34.54	31.76	27.49	22.39	17.15	12.96	8.278	5.241	3.364
	74.47	2.139	4.774	9.027	14.49	20.38	25.66	29.32	30.75	29.89	27.14	23.17	18.67	14.18	10.09	6.690	4.142	2.569
	84.07	1.920	4.362	8.210	13.00	17.92	22.08	24.69	25.37	24.23	21.70	18.33	14.66	10.87	7.826	5.133	3.119	1.874
	94.25	1.605	3.697	6.916	10.78	14.59	17.61	19.30	19.47	18.32	16.23	13.61	10.83	8.140	5.728	3.725	2.226	1.300
	105.02	1.251	2.905	5.390	8.273	10.99	13.01	13.99	13.90	12.92	11.35	9.471	7.512	5.631	3.946	2.545	1.499	0.8520
	116.36	0.9095	2.115	3.884	5.867	7.652	8.888	9.400	9.213	8.486	7.416	6.174	4.937	3.655	2.549	1.632	0.9471	0.5254
	128.29	0.6181	1.426	2.585	3.840	4.917	5.613	5.850	5.674	5.195	4.528	3.766	2.978	2.220	1.541	0.9779	0.5598	0.3034
	140.80	0.3931	0.8900	1.586	2.315	2.913	3.272	3.369	3.244	2.962	2.582	2.148	1.696	1.259	0.8685	0.5464	0.3086	0.1635
	153.89	0.2343	0.5140	0.8968	1.284	1.587	1.757	1.794	1.722	1.573	1.374	1.144	0.9012	0.6716	0.4560	0.2841	0.1582	0.0820
										Photoprotons								
125	40.06	1.952	3.213	5.071	7.168	9.050	10.27	10.54	9.775	8.190	6.164	4.134	2.449	1.295	0.6786	0.4796	0.5177	0.6208
	46.46	3.183	5.050	7.717	10.58	12.95	14.22	14.08	12.59	10.14	7.304	4.660	2.600	1.266	0.6080	0.4330	0.5119	0.6164
	53.33	4.725	7.313	10.90	14.56	17.32	18.45	17.67	15.26	11.84	8.201	5.007	2.644	1.195	0.5170	0.3549	0.4471	0.5868
	60.68	6.439	9.800	14.32	18.70	21.67	22.42	20.83	17.40	13.05	8.724	5.130	2.595	1.104	0.4255	0.2589	0.3324	0.4504
	68.50	8.101	12.19	17.53	22.42	25.36	25.55	23.04	18.67	13.56	8.786	5.013	2.462	1.007	0.3476	0.1613	0.1903	0.2661
	76.80	9.437	14.10	20.00	25.12	27.78	27.27	23.92	18.82	13.28	8.376	4.672	2.259	0.9110	0.2886	0.0765	0.0494	0.0747
	85.57	10.20	15.18	21.30	26.30	28.48	27.28	23.30	17.83	12.25	7.554	4.148	1.999	0.8138	0.2458	0.0135	...	...
	94.81	10.23	15.22	21.17	25.75	27.32	25.56	21.28	15.87	10.65	6.441	3.506	1.702	0.7102	0.2123	...	...	...
	104.53	9.534	14.21	19.64	23.56	24.53	22.44	18.23	13.27	8.716	5.191	2.816	1.387	0.5985	0.1816	...	...	...
	114.73	8.239	12.36	17.00	20.14	20.60	18.45	14.65	10.43	6.716	3.953	2.147	1.078	0.4816	0.1501	...	...	...
	125.39	6.594	9.994	13.73	16.08	16.18	14.20	11.04	7.692	4.871	2.843	1.551	0.7948	0.3670	0.1177	...	...	...
	136.53	4.869	7.507	10.33	11.99	11.88	10.23	7.792	5.328	3.326	1.930	1.060	0.5548	0.2634	0.0868	...	...	...
	148.15	3.310	5.225	7.226	8.335	8.147	6.897	5.155	3.465	2.137	1.236	0.6855	0.3655	0.1775	0.0597	...	...	...
										Photoneutrons								
	40.06	0.1016	0.4584	1.224	2.594	4.701	7.485	10.61	13.51	15.57	16.36	15.77	14.04	11.57	8.872	6.369	4.380	3.114
	46.46	0.1133	0.6185	1.664	3.464	6.124	9.489	13.08	16.19	18.14	18.55	17.42	15.12	12.17	9.110	6.359	4.221	2.876
	53.33	0.1119	0.7924	2.151	4.399	7.583	11.43	15.30	18.40	20.05	19.96	18.29	15.52	12.23	8.963	6.107	3.922	2.560
	60.68	0.0929	0.9609	2.635	5.294	8.898	13.04	16.96	19.82	21.01	20.39	18.26	15.19	11.76	8.471	5.655	3.526	2.207
	68.50	0.0567	1.101	3.049	6.021	9.870	14.07	17.78	20.20	20.86	19.77	17.35	14.19	10.84	7.698	5.054	3.071	1.847
	76.80	0.0086	1.191	3.327	6.458	10.33	14.32	17.61	19.47	19.62	18.20	15.70	12.66	9.564	6.725	4.358	2.590	1.500
	85.57	...	1.217	3.421	6.525	10.19	13.76	16.46	17.74	17.47	15.90	13.52	10.79	8.083	5.641	3.617	2.109	1.181
	94.81	...	1.174	3.309	6.202	9.455	12.44	14.50	15.25	14.71	13.18	11.08	8.769	6.530	4.530	2.879	1.651	0.8953
	104.53	...	1.070	3.012	5.541	8.251	10.58	12.03	12.38	11.72	10.36	8.628	6.792	5.035	3.474	2.190	1.237	0.6516
	114.73	...	0.9226	2.577	4.649	6.761	8.457	9.393	9.473	8.832	7.723	6.387	5.005	3.695	2.536	1.586	0.8831	0.4528
	125.39	...	0.7525	2.071	3.661	5.199	6.349	6.900	6.834	6.290	5.455	4.489	3.504	2.575	1.757	1.089	0.5983	0.2991
	136.53	...	0.5812	1.564	2.702	3.748	4.473	4.763	4.645	4.232	3.649	2.992	2.327	1.701	1.153	0.7079	0.3834	0.1871
	148.15	...	0.4255	1.108	1.869	2.531	2.954	3.089	2.974	2.690	2.311	1.889	1.463	1.063	0.7144	0.4342	0.2319	0.1106

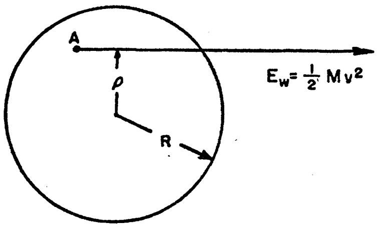

FIG. 3. Path of a photoparticle whose origin is at the point A in the nuclear fluid.

but is likely to collide with other nucleons with the result that the nucleus as a whole is excited. Further, we neglect refraction of the photoparticles in crossing the change in nuclear potential. This means that we neglect distortion of the photoparticle angular distribution developed in the last section, but expect that the energy spectrum will be modified.

The nuclear model considered is a sphere of uniformly distributed nuclear fluid which gives rise to a square potential well. In Fig. 3, we show such a nucleus and the path of a photoparticle whose origin is at the point A. This photoparticle has an angular momentum $Mv\rho$. From the standpoint of quantum mechanics, its square is given by $(Mv\rho)^2 = l(l+1)\hbar^2$, where l is an integer. For 100-Mev photoparticles in a carbon nucleus, the largest value of l that occurs is about 8. For photoparticles with energies E_w measured above the bottom of the nuclear well, the yield of photoparticles which escape from the nucleus is given by;

$$I(E_w) = \sum_{l=0}^{l_{\max}} P_l T_l(E_w), \tag{16}$$

where P_l is the probability of occurrence of l, and $T_l(E_w)$ is the probability of escape from the nucleus of photoparticles with energy E_w and angular momentum quantum number l. The upper limit on the summation, $l_{\max}$, is the maximum value of l that occurs with given E_w and nuclear radius R.

The probability $T_l(E_w)$ may be calculated using[25]

$$T_l(E_w) = 4S_l KR / [\Delta_l^2 + (S_l + KR)^2],$$

where K is the wave number of the particle inside the nucleus associated with the energy E_w, and $(\Delta_l + iS_l)$ is the logarithmic derivative of the wave function of the photoparticle evaluated at the nuclear surface. Δ_l and S_l are given in terms of the regular and irregular Coulomb wave function F_l and G_l. The asymptotic expressions for F_l and G_l are respectively the real and imaginary parts of[26]

$$i \exp\{-i[kr - n\ln(2kr) - l\pi/2 + \eta_l]\} \times g(-l-in, l+1-in, -2ikr),$$

where

$$g(\alpha,\beta,z) = 1 + \frac{\alpha\beta}{z} + \frac{\alpha(\alpha+1)\beta(\beta+1)}{2!z^2} + \cdots,$$

and

$$\eta_l = \arg\Gamma(l+1+in).$$

The parameter n is defined by Ze^2/hv, where v is the velocity of the particle outside the nucleus and k is the associated wave number. Three terms of the above series for $g(-l-in, l+1-in, -2ikr)$ are sufficient for our use as the expansion parameter $z = -2ikr$ evaluated at the nuclear radius R is large for the values of k encountered. Numerical substitutions in the resulting expression for T_l may be compared with the results obtained using the tables of Coulomb wave functions of Bloch *et al.*[27] In a particular case which provides a severe test of our formula for T_l, it is found that our results are a few percent high[28] for $l=0$ and $l=1$.

Since several values of l occur in the sum in Eq. (16), the sum may be approximated by an integral over ρ, where $(Mv\rho)^2 = l(l+1)\hbar^2$ is used. Equation (16) becomes

$$I(E_w) \cong \int_0^R P(\rho) T(\rho, E_w) d\rho, \tag{17}$$

where $T(\rho,E_w)$ is $T_l(E_w)$ in which $l(l+1)$ has been replaced by $(Mv\rho/\hbar)^2$. The function $P(\rho)d\rho$ is the probability that ρ lies between ρ and $\rho+d\rho$.

Since the nucleons comprising the nucleus are assumed to be distributed uniformly within a sphere of radius R, we see that $P(\rho) = (3/R^3)\rho(R^2-\rho^2)^{\frac{1}{2}}$. There is a value ρ_0 of ρ at which the total Coulomb plus centrifugal barrier is equal to the laboratory energy $E_L = E_w - V$ of the photoparticle. For $R > \rho > \rho_0$, the penetrability $T(\rho,E_w)$ is small, and it can be shown[29] that for cases of interest, the contribution of the integral (17) from this region is small also and may be neglected. The integration may be done exactly and gives the average transmission probability for photoneutrons and photoprotons formed in the nucleus. Numerical work based on the resulting formula is given

TABLE II. Average proton barrier penetration probabilities for the carbon nucleus calculated by using a nuclear potential well depth of 40 Mev and 3.2×10^{-13} cm for the radius of the carbon nucleus.

Lab proton energy E_L (Mev)	Average penetration probability
10	0.5953
20	0.7924
30	0.8675
40	0.9052
50	0.9280
60	0.9425
70	0.9525
80	0.9600
90	0.9654
100	0.9661

[25] Reference 12, p. 360.
[26] Reference 11, p. 116.

[27] Block, Hull, Broyles, Bouricius, Freeman, and Breit, Revs. Modern Phys. 23, 147 (1951).
[28] There is an error in Fig. 5.3 (p. 363) in reference 12. The T_l are shown much too small.
[29] See reference 17, p. 66.

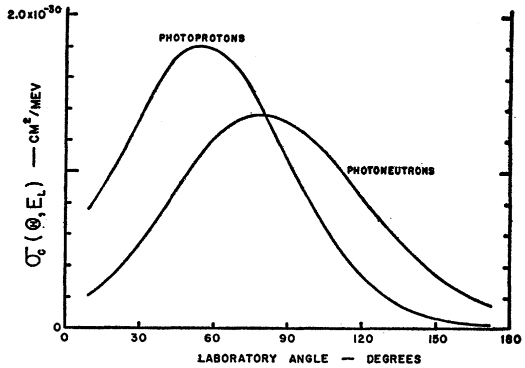

FIG. 4. The theoretical angular distributions of photoprotons and photoneutrons with laboratory energies $E_L=23.6$ Mev, from carbon irradiated by 75-Mev photons.

in Table II in the case of the carbon nucleus with a nuclear potential well depth of 40 Mev.

V. NUMERICAL RESULTS

The cross section $\sigma(\Theta,E_w)$ given by Eqs. (8) and (13) has been evaluated numerically in the case of the Gaussian ground state nucleon momentum distribution, where the $1/e$ value occurs at 16 Mev. The numerical work[30] is done for four photon energies, *viz.*, 50, 75, 100, and 125 Mev. For each photon energy, the cross section is evaluated at 10° intervals in the laboratory coordinate system and at a variety of values of the photoparticle energy E_w which is the energy taken with the bottom of the nuclear potential well as a reference. The results are presented in Table I and give the value of $v\sigma(\Theta,E_w)$, where v is the nuclear volume. These results are not intended to be descriptive of the photoeffect for a particular nuclide except where the Gaussian ground-state nucleon distribution parameters chosen ($1/e$ value at 16 Mev) represent to a better approximation the momentum distributions in some nuclides than others.

In applying the results of Table I to a particular nucleus, we must divide by the nuclear volume v which may be taken as $(4\pi/3)R^3$, where we may use $R=r_0A^{\frac{1}{3}}$, in which $r_0=1.4\times10^{-13}$ cm and A is the mass number. It is then necessary to multiply by NZ, the number of quasi-deuterons in the nucleus, since the calculation of Sec. III was done for one quasi-deuteron. Finally, the result must be multiplied by the escape probability calculated in Sec. IV.

As an example of the use of the tables, consider the photoeffect in carbon irradiated by 75-Mev photons. We calculate the angle distributions of 23.6-Mev photoprotons and photoneutrons and the energy distribution of photoprotons at the laboratory angle of 60°. The results are given in Figs. 4 and 5, respectively. To obtain the angle distributions of Fig. 4, we enter Table I with a photon energy of 75 Mev, and with an E_w value of $(40+23.6)=63.6$ Mev for both photoprotons and photoneutrons. The tabulated values are then multiplied by $(NZ/v)=2.61\times10^{38}$ cm^{-3}. In the case of protons, we then multiply by the value of the proton barrier penetration probability (0.825) which is obtained by graphically interpolating between values given in Table II. For neutrons, we multiply by (0.875) which is the appropriate barrier penetration probability. The energy distribution of 60° photoprotons of Fig. 5 is obtained from Tables I and II in essentially the same way.

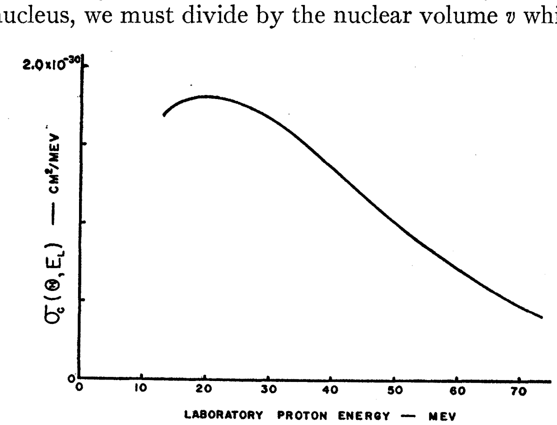

FIG. 5. The theoretical energy spectrum of photoprotons from carbon irradiated by 75-Mev photons. The yield is taken at a laboratory angle of 60°.

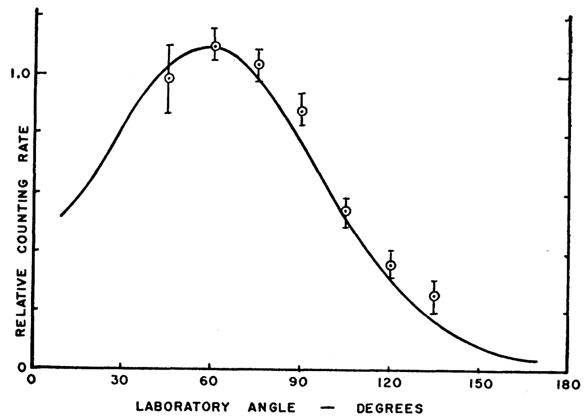

FIG. 6. Experimental data of Johansson[31] showing the yield of photoprotons with energies greater than 14 Mev obtained from carbon irradiated by the bremsstrahlung beam from a betatron operating at 65 Mev. The smooth curve is the calculated yield of 13.3-Mev photoprotons from carbon irradiated by 50-Mev photons. The normalization is at 60°.

VI. DISCUSSION

Experimental data which allow a detailed check of the calculations presented here are not available at present. In most experiments, the bremsstrahlung beam from a betatron or electron synchrotron is used and so the photoparticle yield is from many photon energies. The experimental apparatus of Weil and McDaniel[5] counts only those events due to 190-Mev photons out of a bremsstrahlung beam, and any data that may be taken in the future using a method such as theirs should

[30] The numerical work was performed on the I.B.M. Card-Programmed Calculator of the Stanford Computation Center.

be very helpful in making a critical evaluation of our photoeffect calculations.

No numerical work was done at photon energies as high as 190 Mev and so comparison with the data of Weil and McDaniel is not possible. The bremsstrahlung experiment of Johansson[31] at 65 Mev is of interest since both photoneutrons and photoprotons which had reasonably well defined laboratory energies were observed. The angular distribution of the yield of photoprotons having energies greater than 14 Mev from carbon as observed by Johansson is shown in Fig. 6. By way of comparison, there is shown also on Fig. 6, our calculated results for 13.3-Mev photoprotons from carbon irradiated by 50-Mev photons. The two curves are normalized at 60° laboratory angle. In the case of photoneutrons, Johansson obtained no data for carbon, but did notice in the cases of Be, Al, Ta, and Tb, that neutrons were emitted preferentially at 90° in the laboratory. This agrees qualitatively with our results for photoneutrons, as may be seen in Fig. 4.

As more experimental data become available, it might be of interest to test deuteron-model calculation using a variety of ground-state nucleon momentum distributions and then see if the same momentum distributions that give the best agreement in the case of the nuclear photoeffect also give the best agreement for proton scattering[7] and the "pickup" process.[9]

[31] S. A. E. Johansson, Phys. Rev. 97, 434 (1955).

ACKNOWLEDGMENTS

I wish to thank Professor L. I. Schiff for his very helpful advice in many parts of this calculation.

PHYSICAL REVIEW VOLUME 100, NUMBER 1 OCTOBER 1, 1955

Gamma-Gamma Angular Correlation in Ba^{134}

ERNEST D. KLEMA
Oak Ridge National Laboratory, Oak Ridge, Tennessee
(Received May 20, 1955)

The directional angular correlation of the 1367–605 kev γ-γ cascade in Ba^{134} has been measured with a coincidence scintillation spectrometer using NaI detectors. For a dilute cesium chloride aqueous solution source, the observed correlation function, after correcting for the finite angular resolution of the detectors, is given by $W(\theta)=1+(0.090\pm0.0086)P_2(\cos\theta)-(0.004\pm0.013)P_4(\cos\theta)$. From this result it is not possible to assign unambiguously a spin and parity to the 1972-kev level in Ba^{134}, from which the cascade originates. However, the present angular correlation data taken with internal conversion coefficient data for the transitions from this level indicate that it very probably has spin 3 and odd parity.

I. EXPERIMENTAL RESULTS

THE directional angular correlation of the 1367–605 kev γ-γ cascade in Ba^{134} has been measured with a coincidence scintillation spectrometer using NaI detectors in a series of 5 experiments with a total of 1.1×10^5 coincidence counts taken at 19 angular positions. The source was a dilute aqueous solution of cesium chloride.

The data were obtained as discussed previously[1] and were analyzed following the paper of Rose.[2] The γ-ray spectrum of the cesium chloride source is shown in Fig. 1. Each point on the curve out to a pulse height of 810 units contains 4096 counts, and the points for greater pulse heights contain 1024 counts each. The windows of the differential pulse-height analyzers were placed, as shown in Fig. 1, so that one was set on the full-energy peak of the 605-kev γ ray and the other accepted only the full-energy peak of the 1367-kev γ ray. Since the latter γ ray is the highest-energy one of the source, the measurement of the angular correlation of the 1367–605 kev cascade is a clean one and needs no correction for interference by the other cascades.

The true coincidence counting rate for the present experiment was of the order of 3.5×10^{-2} count/sec and the random rate was 15% of this. The correlation function obtained, after correcting for the finite angular resolution of the detectors, is

$$W(\theta)=1+(0.090\pm0.0086)P_2(\cos\theta)-(0.004\pm0.013)P_4(\cos\theta).$$

The errors given above are the standard deviations as defined by Eq. (30) of Rose's[2] paper.

II. ANALYSIS OF RESULTS

The most recent decay scheme proposed for Cs^{134} is given in Fig. 2.[3] In contrast with the ones previously advanced, it agrees with coincidence data obtained at this laboratory and with the relative intensities of the γ rays as measured by scintillation spectrometry here.[4]

[1] E. D. Klema and F. K. McGowan, Phys. Rev. 91, 616 (1953).
[2] M. E. Rose, Phys. Rev. 91, 610 (1953).
[3] Keister, Lee, and Schmidt, Phys. Rev. 97, 451 (1955).
[4] R. C. Davis, private communication.